1. Report No. ATC-189	2. Government Accession No. DOT/FAA/NR-92/7	3. Recipient's Catalog No.
4. Title and Subtitle Airport Surveillance Radar (ASR-9) Wind Shear Processor: 1991 Test at Orlando, FL		5. Report Date 1 June 1992
		6. Performing Organization Code
7. Author(s) Mark E. Weber		8. Performing Organization Report No. ATC-189
9. Performing Organization Name and Address Lincoln Laboratory, MIT P.O. Box 73 Lexington, MA 02173-9108		10. Work Unit No. (TRAIS)
		11. Contract or Grant No. DTFA-01-89-Z-02030
12. Sponsoring Agency Name and Address Department of Transportation Federal Aviation Administration Systems Research and Development Service Washington, DC 20591		13. Type of Report and Period Covered Project Report
		14. Sponsoring Agency Code

15. Supplementary Notes

16. Abstract

An operational test of a Wind Shear Processor (WSP) add-on to the Federal Aviation Administration's airport surveillance radar (ASR-9) took place at Orlando International Airport during July and August 1991. The test allowed for both quantitative assessment of the WSP's signal processing and wind shear detection algorithms and for feedback from air traffic controllers and their supervisors on the strengths and weaknesses of the system. Thunderstorm activity during the test period was intense; low-altitude wind shear impacted the runways or approach/departure corridors on 40 of the 53 test days. As in previous evaluations of the WSP in the southeastern United States, microburst detection performance was very reliable. Over 95% of the strong microbursts that affected the Orlando airport during the test period were detected by the system. Gust front detection during the test, while operationally useful, was not as reliable as it should have been, given the quality of gust front signatures in the base reflectivity and radial velocity data from the WSP. Subsequent development of a "Machine Intelligent" gust front algorithm has resulted in significantly improved detection capability. Results from the operational test are being utilized in ongoing refinement of the WSP.

17. Key Words		18. Distribution Statement
airport surveillance radar microburst air traffic control	wind shear processor gust front	This document is available to the public through the National Technical Information Service, Springfield, VA 22161.

19. Security Classif. (of this report) Unclassified	20. Security Classif. (of this page) Unclassified	21. No. of Pages 48	22. Price

FORM DOT F 1700.7 (8-72)   Reproduction of completed page authorized

ABSTRACT

An operational test of a Wind Shear Processor (WSP) add–on to the Federal Aviation Administration's airport surveillance radar (ASR–9) took place at Orlando International Airport during July and August 1991. The test allowed for both quantitative assessment of the WSP's signal processing and wind shear detection algorithms and for feedback from air traffic controllers and their supervisors on the strengths and weaknesses of the system. Thunderstorm activity during the test period was intense; low altitude wind shear impacted the runways or approach/departure corridors on 40 of the 53 test days. As in previous evaluations of the WSP in the southeastern United States, microburst detection performance was very reliable. Over 95% of the strong microbursts (> 30 knots) that affected the Orlando airport during the test period were detected by the system. Gust front detection during the test, while operationally useful, was not as reliable as it should have been, given the quality of gust front signatures in the base reflectivity and radial velocity data from the WSP. Subsequent development of a "Machine Intelligent" gust front algorithm has resulted in significantly improved detection capability. Results from the operational test are being utilized in ongoing refinement of the WSP.

ACKNOWLEDGMENTS

TABLE OF CONTENTS

LIST OF ILLUSTRATIONS

LIST OF TABLES

1. INTRODUCTION

An operational test of a Wind Shear Processor (WSP) add–on to the Airport Surveillance Radar (ASR–9) was conducted at the Orlando International Airport (MCO) during July and August of 1991. The test followed a similar evaluation of the WSP in 1990 [1] and featured augmented range coverage, improved meteorological hazard detection algorithms, and use of a production ASR–9 in place of the ASR–8 testbed used previously. This report describes the experimental WSP, the test conditions and an assessment of the WSP's performance during the operational evaluation.

The WSP has been under development since 1985, under sponsorship by the Federal Aviation Administration's ASR–9 Program Office. [2] When implemented nationally, the WSP will provide broad–area wind shear detection capability at smaller airports not slated to receive a dedicated Terminal Doppler Weather Radar (TDWR). [3] Based on a recently completed windshear detection systems cost–benefit study, [4] the FAA plans to deploy 58 WSP systems; 35 in a stand–alone mode and 23 in an integrated configuration with the Enhanced Low Level Windshear Alert System (LLWAS). [5] The WSP procurement is nominally scheduled to begin in 1994.

The 1991 operational test was conducted to validate the operational utility of the WSP and to obtain data necessary to continue system refinement. The evaluation had two components:

1. Quantitative assessment of the performance of the WSP's signal processing and wind shear detection algorithms in the moist, convectively unstable environment of the Florida peninsula; and

2. Feedback from users (air traffic controllers and supervisors) on strengths and weaknesses of the system and their recommendations for modifications.

The first objective was achieved by recording wind shear alarms generated by the WSP and correlating these off line with observations from the other meteorological sensing systems described in Section 2. User feedback was obtained through periodic meetings with air traffic control personnel using the system at the Orlando facility. The results of the operational test are being utilized in ongoing refinement of the WSP system.

Section 2 of this report provides an overview of the testbed WSP and the other sensors used to document low altitude wind shear and other weather phenomena. Sections 3 reviews the 1991 operational test and the performance of the WSP. Details on the data processing algorithms are contained in the appendices.

1

2. ORLANDO WSP TESTBED

Figure 1 is a high level block diagram of the Wind Shear Processor testbed as operated in 1991. The system is comprised of:

1. A production ASR-9;

2. Interfaces to extract necessary RF and timing signals;

3. Identical high dynamic range receivers and A/D converters for the high and low beam receiving channels of the ASR-9;

4. A digital signal processor that performs signal pre-conditioning (e.g., ground clutter filtering) and computes estimates of the precipitation reflectivity factor, low-altitude radial velocity and spectrum width in each range-azimuth resolution cell;

5. A high-density digital recorder to archive unprocessed in phase and quadrature (I and Q) signals from both receiving beams;

6. Local workstations that run the microburst and gust front detection algorithms, the storm motion algorithm, generate precipitation reflectivity maps, and transmit the resulting products to the air traffic control tower; and

7. Remote workstations and monitors that provide graphical and alphanumeric displays to air traffic controllers and their supervisors.

Figure 2 is a photograph of the test site on the Orlando airport. Both channels of the ASR-9 (transmit and receive cabinets, target processors, six-level weather processors and RMS) are deployed in the mobile five-foot trailer in the foreground. This trailer also houses the signal interface module, receivers and A/D converters for the WSP. Digitized signals are transmitted over a fiber optic link to the adjacent office trailer which contains the data processing and recording system.

2.1 WSP RADAR INTERFACES AND RECEIVERS

As indicated in Figure 1, the WSP requires simultaneous access to both high and low receiving beams in order to accurately calculate the low-altitude radial wind field. [2] In order to generate identical RF paths for both beams, the ASR-9's high/low-beam switch was bypassed and an additional band pass filter and low noise amplifier were added. This provided identical paths for both beam channels to the WSP receivers. In the production implementation for the WSP, a network of switches and RF couplers will be employed so as to provide signals simultaneously to the WSP and the ASR-9's target and six-level weather processors. [2]

The WSP receivers (Figure 3) are double conversion receivers with digital automatic gain control (AGC) in the IF stage and quadrature video detectors providing baseband output. The stable local oscillator (STALO) and coherent local oscillator (COHO) signals are
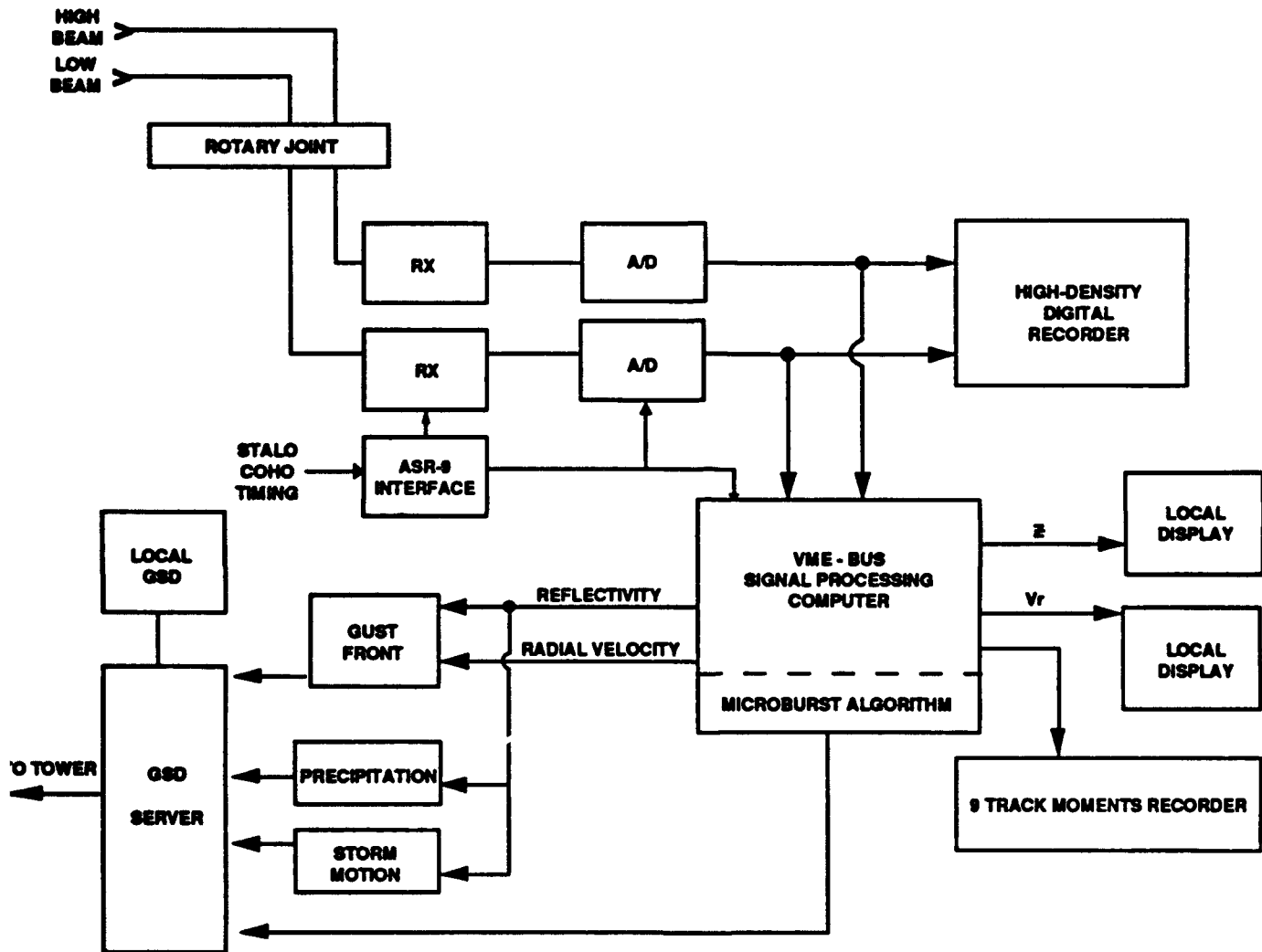
3

Figure 1. High-level block diagram of the 1991 Orlando ASR-9 Wind Shear Processor testbed.
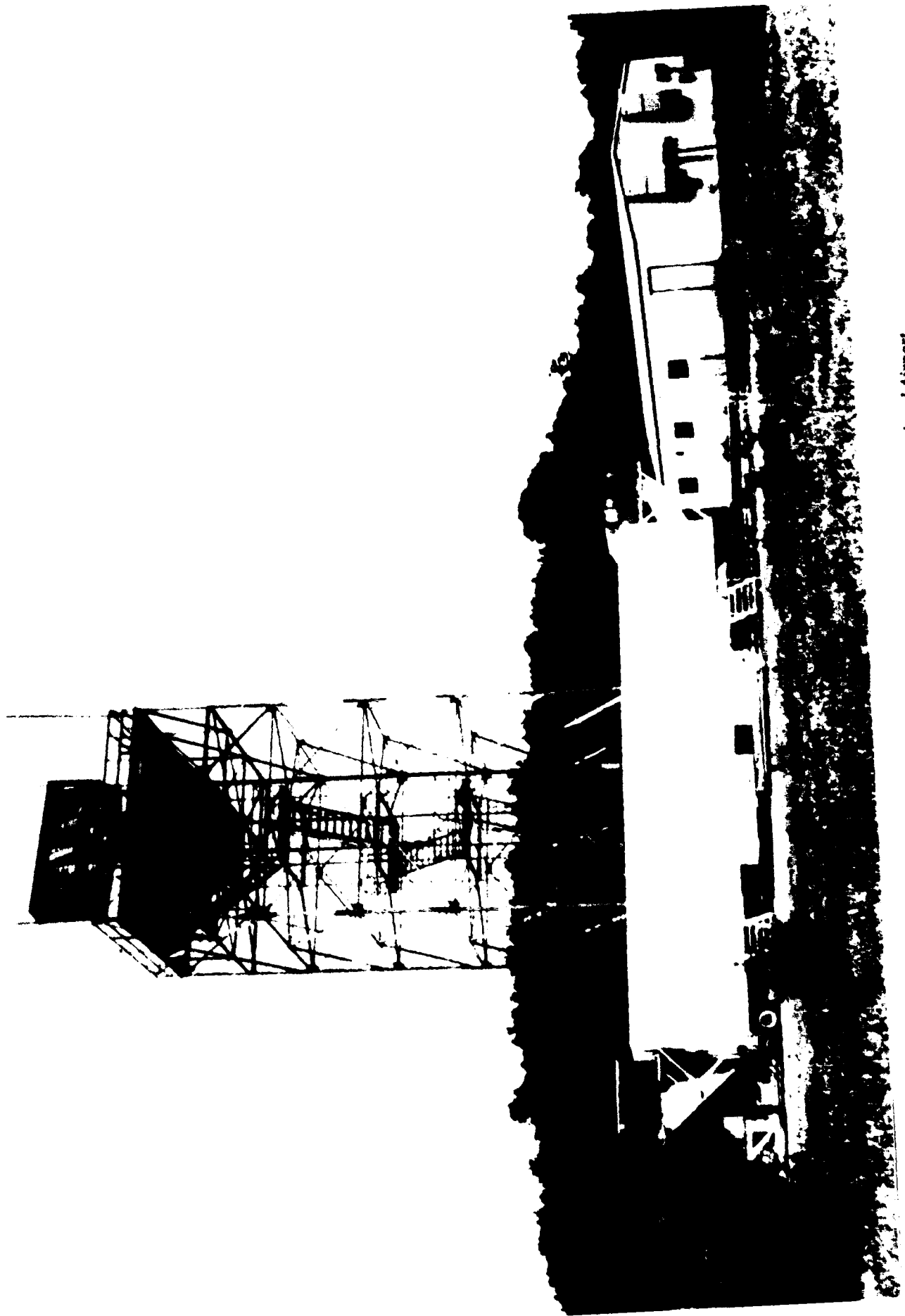
Figure 2. Photograph of ASR-9 Wind Shear Processor testbed on Orlando International Airport.

5
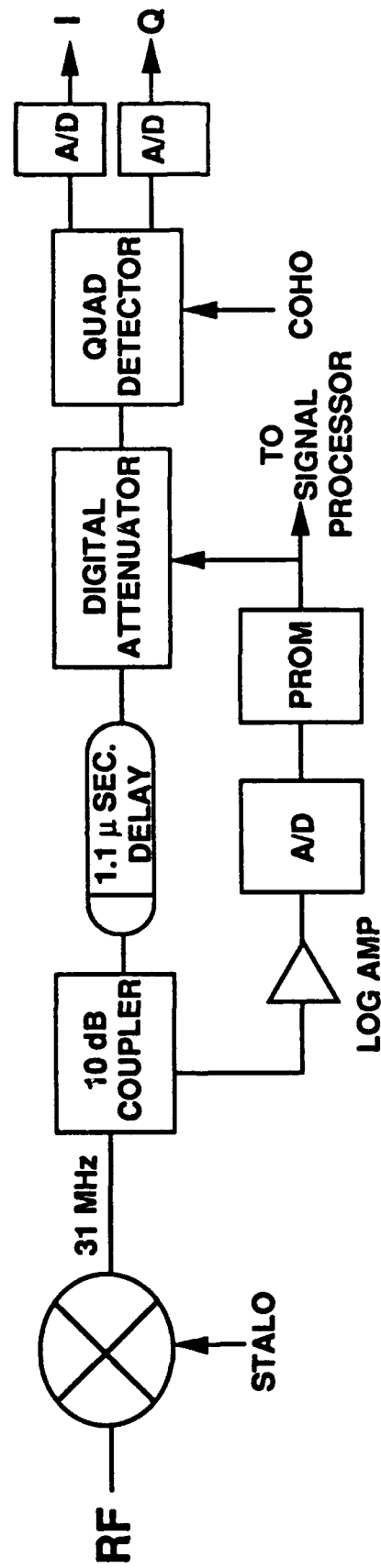
Figure 3. Wind Shear Processor receivers.

tapped from the ASR−9 and are isolated from the radar by circulators. The IF signal (at 31.1 MHz) is split into two paths in order to implement the AGC. One path is through a linear channel with 1.1 microsecond delay introduced by means of a coaxial delay line. The other path is through a logarithmic amplifier whose output is sampled at a 10.35 MHz rate by an eight−bit flash A/D converter. A PROM converts the highest flash−conversion sample from each radar range gate (773 ns or 1/16 nmi) to an attenuation factor which varies from 0 to 45 dB in 3 dB increments. This factor drives a digital PIN diode attenuator at the output of the linear channel delay line so that the IF signal will not exceed the dynamic range of the A/D converters in the quadrature video detection stage. The attenuation factor for each range gate is supplied to the digital signal processor along with the corresponding in phase and quadrature samples so that the appropriate corrections to signal amplitude can be implemented. The quadrature video detector employs 14 bit A/D convertors so that total system dynamic range is 129 dB. In addition to STALO and COHO signals, the WSP signal interface module extracts the following digital signals from the ASR−9:

1. 10.35 MHz clock

2. 1.29 MHz range−gate clock

3. Azimuth change pulse (ACP)

4. Azimuth reference pulse (ARP)

5. Transmitter pre−trigger

Data for each pulse transmitted by the radar are packaged as a "record" consisting of eight 32−bit "header" words containing status information such as time, antenna azimuth, pulse repetition interval (PRI), etc., followed by two 32−bit words for each range gate. These encode the in phase and quadrature samples for both receiving channels along with the corresponding AGC attenuation factor.

2.2 DIGITAL PROCESSOR AND RECORDING SYSTEM

In phase and quadrature samples and ancillary data are transmitted via fiber optic link to a Radar Data Bus in the processing and display trailer. This 50−conductor ribbon cable supplies data simultaneously to the high−density digital recorder and the signal−processing computer.

The signal processing computer operates as a loosely coupled multiprocessor, incorporating several single−board computing systems connected by VME busses. A data input processor (a Mercury MC3200 processor) receives the incoming I and Q samples and distributes these to six signal processing boards (Mercury MC860 processors). Each of these boards performs the full suite of signal processing operations on a specific interval of range gates. The output products (reflectivity, radial velocity, spectrum width and signal−to−noise ratio) are reassembled by an output processor and passed on to the meteorological detection algorithms.

8

The microburst algorithm was implemented on a single—board computer on this same VME backplane. For convenience, the gust front, storm motion and six—level precipitation algorithms were implemented on UNIX workstations (SUN3 and SUN4) connected via an ethernet LAN. In a production WSP, these outboard workstations would probably be replaced by additional single—board computers in order to minimize processor size and expense.

2.3 USER DISPLAYS

Figures 4a and 4b show the graphical and alphanumeric displays provided to air traffic controllers at the Orlando FAA facility. The displays, products and operational procedures for using these products are essentially identical to those developed for the TDWR.

The color workstation, a Geographic Situation Display (GSD) was provided for the area managers in the Terminal Radar Control Room (TRACON) and tower cab. This device gives graphical representations of the location and intensity of precipitation, microbursts and gust fronts as well as estimates of the speed and direction of motion for precipitation cells and gust fronts. When wind shear events intersect active runways or approach/departure corridors, runway specific alphanumeric messages are generated on the "ribbon" display. These are read off by the local controller when planes are cleared for takeoff or final approach. Reference [1] provides more detailed information on the user interfaces and operational procedures.

2.4 SUPPORTING SENSORS

Figure 5 shows the additional meteorological sensors deployed near the Orlando airport during the operational test period. Lincoln Laboratory's TDWR testbed, the University of North Dakota's C—Band radar, and the MIT Weather Radar Laboratory's C—Band radar provided a short baseline triple—Doppler network that allows for reconstruction of the full wind vector in thunderstorms occurring near the airport. Data from these radars were used for quantitative scoring of the WSP's microburst and gust front detection algorithms. A ME-SONET consisting of Orlando airport's 15—station enhanced LLWAS and an additional 15 anemometers deployed by Lincoln Laboratory provided dense surface wind measurements in the vicinity of MCO. The anemometer network, in addition to providing another source of "truth" for the WSP's algorithms assessment, was used for the initial evaluation of WSP/En-hanced LLWAS integration discussed in Appendix B. Note that the Orlando Enhanced LLWAS was not commissioned during 1991; therefore, the integration algorithm evaluation was conducted off line. A two—station interferometric lightning detection and localization system was deployed and operated by the French Government Laboratory ONERA. Data on in-tracloud and cloud to ground lightning activity obtained with this system are being analyzed to develop applications for aviation weather hazard detection.

9
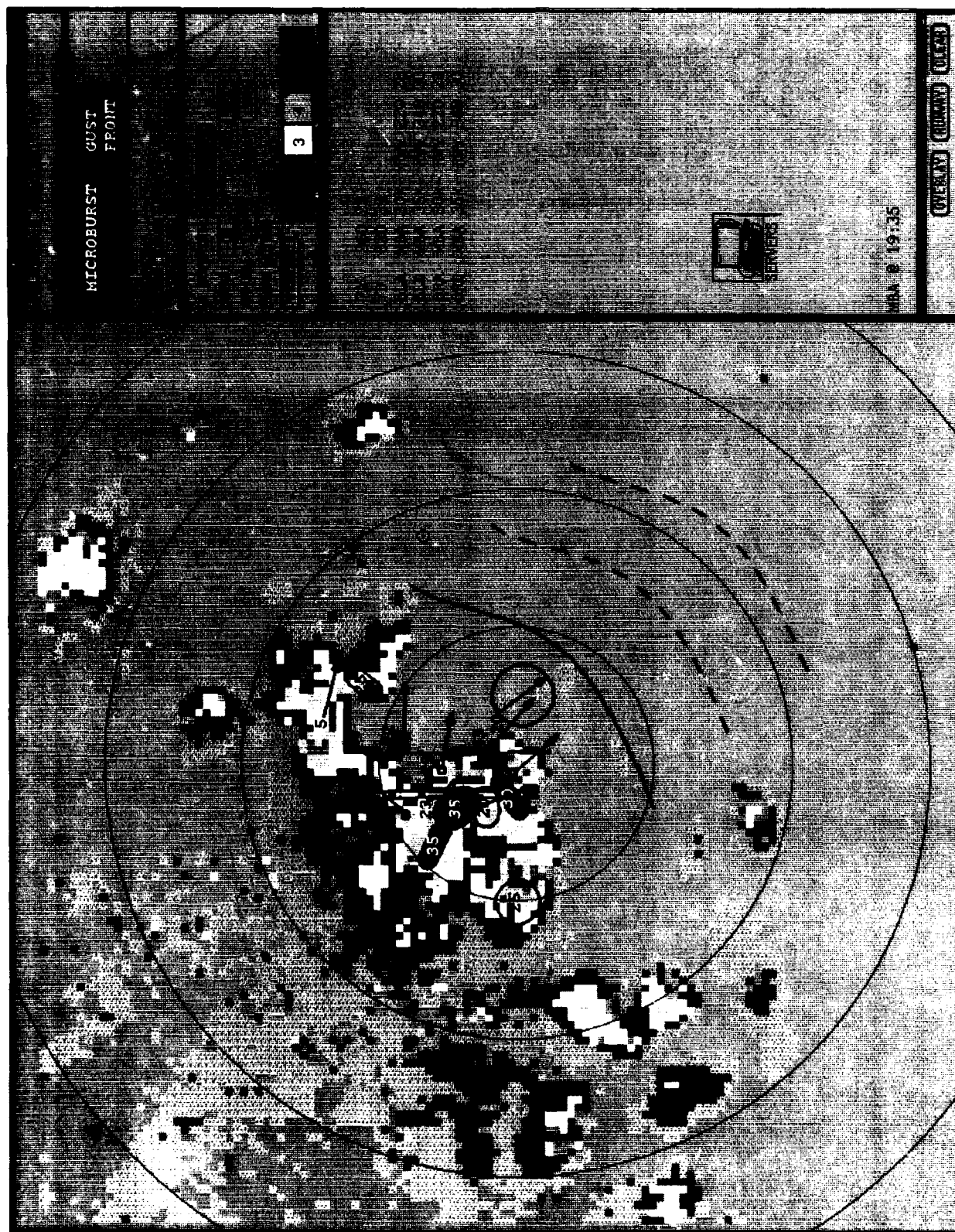
Figure 4a. Geographic Situation Display. Filled red circles are detected microbursts with the measured wind changes across the event (in knots) indicated. Open red circles show divergent outflows with measured wind changes less than 30 knots ("wind shear with loss"). Purple arc is a detected gust front with the estimated location of the front 10 and 20 minutes in the future indicated by dashed purple lines; an estimate of the wind speed and direction behind the front is given by the purple vector. Six levels of precipitation reflectivity are shown and the speed and direction of storm movement is given by the black vector and associated number. The blue arrows and numbers show the wind speed and direction measured by LLWAS S anemometers.

11
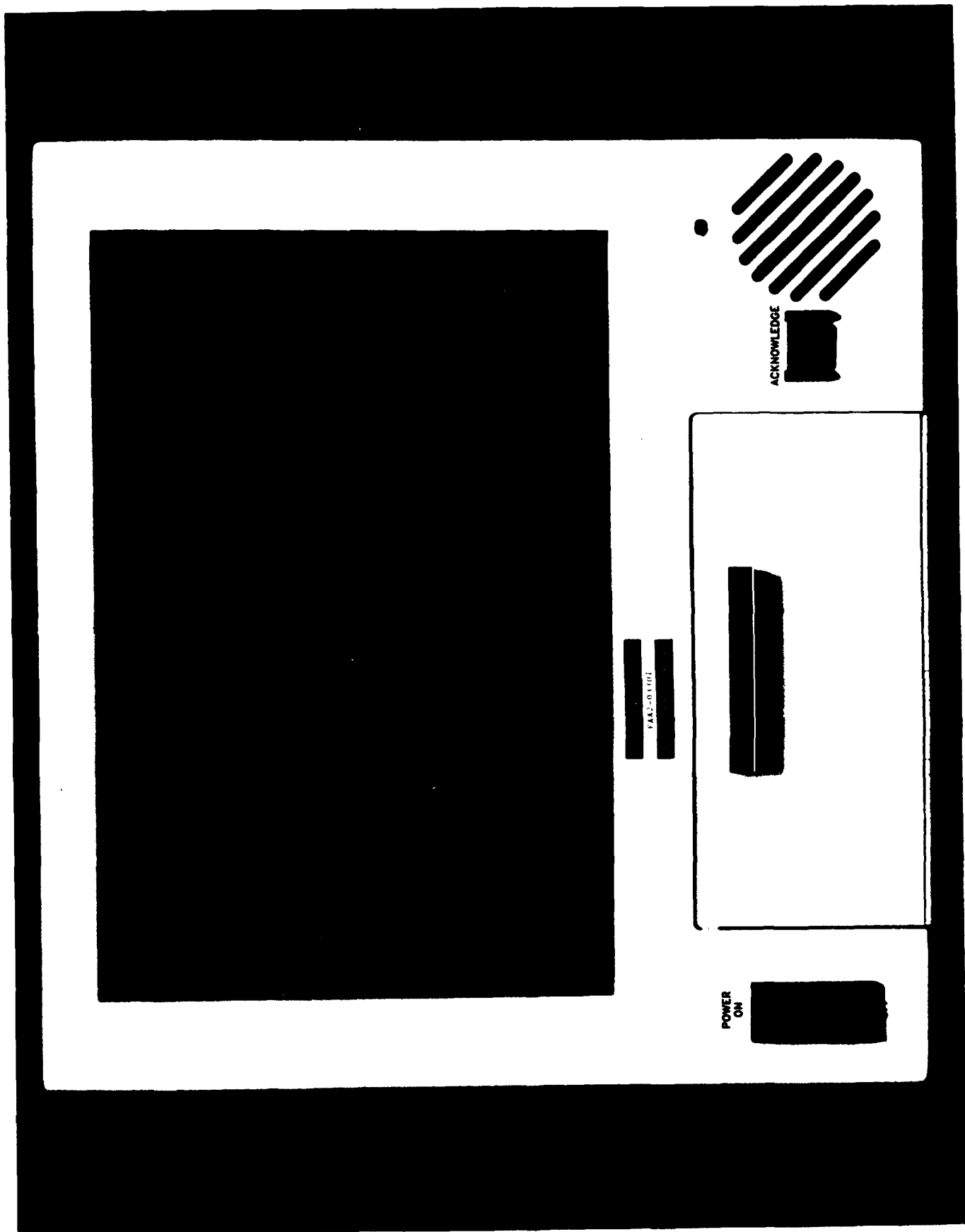
Figure 4b. Alphanumeric ("ribbon") display. The first line is read as "microburst alert on runway 17 arrival, 30 knot loss at 1 mile final, threshold winds 11 knots from 150 degrees."

13

WINDSHEAR DETECTION
RADAR LOCATIONS FOR
1990/1991 TESTS IN ORLANDO

1 MILE

LLWAS

UND

MIT

ASR

TDWR

L
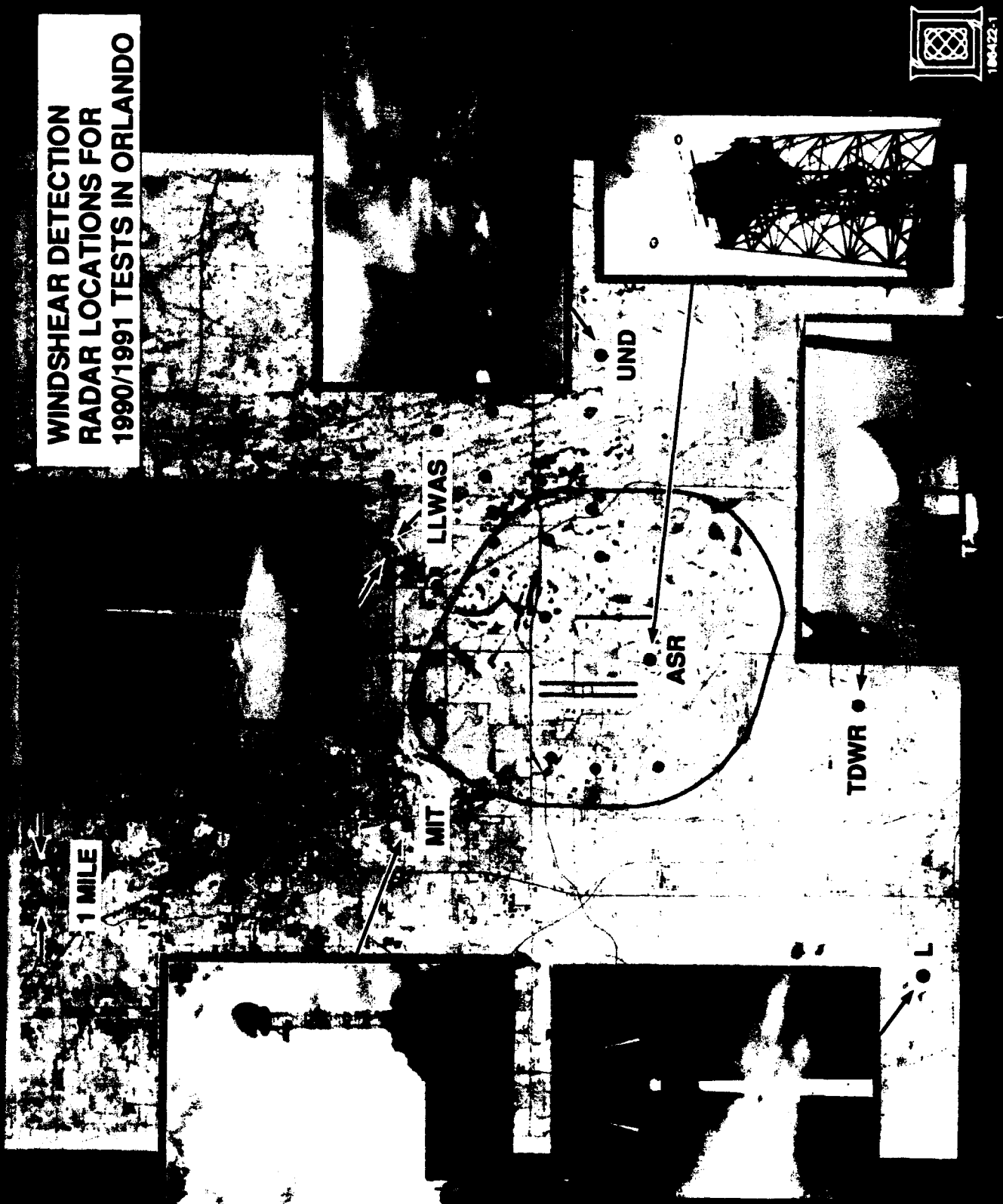
Figure 5. Map showing locations of Doppler radars, anemometers, and lightning detection system (L) relative to Orlando International Airport. The vertical black lines in the center of the picture are the three parallel runways at the airport.

15

3. SYNOPSIS OF 1991 OPERATIONAL TEST

The 1991 ASR–9 WSP operational test followed a similar evaluation using Lincoln Laboratory's TDWR testbed in May and June. The WSP evaluation took place seven days per week from 10 July to 31 August during the hours 1200 to 1900 EDT. The test period was frequently extended beyond 1900 owing to continued weather activity in the vicinity of MCO. During the two–month operational period, the WSP was inoperable a total of 6.5 hours due to software or hardware failures. This downtime represents less than two percent of the total operating time.

In contrast to the initial WSP test in 1990, thunderstorm activity during the 1991 test period was intense. Low–altitude wind shear impacted the runways or approach/departure corridors at MCO on 40 of the 53 test days. A total of almost 500 microbursts were detected by the WSP, 71 of which impacted the airport. Approximately 50 gust fronts were observed, 31 of which passed over the airport.

3.1 MICROBURST DETECTION PERFORMANCE

Overall, the performance of the WSP's microburst detection function was good, both in terms of quantitative detection and false–alarm statistics and in terms of the favorable assessment of this function by Orlando's air traffic control team. Implementation of more precise fitting of user–displayed microburst shapes to the actual region of strong shear and incorporation of a "shear integration" technique in the generation of alphanumeric alarm messages largely eliminated the sense of "overwarning" that had been voiced by Orlando air traffic controllers during the 1990 TDWR and WSP tests.

Two statistical scoring methodologies were employed to quantify the performance of the WSP's microburst detection function. "Hit–miss" scoring tabulates whether microburst alarm regions generated by the WSP intersected "true" microbursts. If any overlap existed, the WSP alarm was scored as a detection; otherwise, it was deemed to be a false alarm. "True" microbursts were identified based on manual examination of single–Doppler data from the TDWR testbed.

Table 1 tabulates hit–miss detection and false–alarm probabilities for 11 days during the operational demonstration (10, 11, 17, 28, 29 July and 1, 2, 9, 10, 15, 31 August). These days included the most active weather periods during the operational period. The data set contains a total of almost 9000 single–scan observations of microburst events. Only wind shear events within 12 km of the radar (the region of operational significance for an ASR–9 WSP) were included in the analysis. The statistics are tabulated separately for all "wind shears with loss" (divergences with total loss greater than 15 kts), "microbursts" (total loss greater than 30 kts) and "strong microbursts" (total loss greater than 40 kts).

TABLE 1.
MICROBURST ALGORITHM HIT-MISS SCORING STATISTICS

	Probability of Detection	Probability of False Alarm
Wind Shear with Loss	0.94	0.23
Microburst	0.98	0.08
Strong Microburst	1.00	0.01

As with previous evaluations of the WSP in the southeastern United States, the detection probability for microbursts was well above the 90% criterion established for the TDWR in its Systems Requirement Statement (SRS). The false−alarm probability was low for "microburst" strength divergences, but increased significantly within the "wind shear with loss" category. Most of the false alarms in this category had reported losses in the 15 to 25 kt range. The higher incidence of "wind shear with loss" false alarms was not reported as a problem by the Orlando air traffic controllers. (The alarms were almost always associated with heavy precipitation and gusty winds; thus, air traffic operations were normally curtailed for other reasons.)

"Path−oriented" scoring quantified the accuracy of the WSP's alphanumeric alarms relative to the actual loss that would have been experienced by a landing or departing aircraft on one of MCO's runways. For this analysis "truth" was determined using a dual−Doppler analysis of the surface wind field from TDWR and UND radar measurements. For each runway, the integrated loss measured along the approach and departure corridors was computed and correlated with the WSP's alarms for that runway. In general, path−oriented scoring provides a more stringent performance assessment than hit−miss statistics; good performance with this metric requires reliable detection, accurate localization and accurate strength characterization for the wind shear event.

Table 2 lists various performance metrics derived from the path−oriented scoring. Data from nine days during the operational demonstration (coinciding with time periods for a similar analysis of TDWR and enhanced LLWAS system performance) were analyzed. The analysis periods included approximately 8000 single−scan observations of microbursts (loss greater than 30 kts), 12000 observations of weaker divergences (loss between 20 and 30 kts), and 60,000 null observations (no true wind shear events near MCO). The detection metrics are given as conditional probabilities. Thus P(LOSS | MB) is the probability that the WSP reported a "wind shear with loss" or "microburst" given that the dual−Doppler analysis indicated an airplane would have experienced "microburst" strength shear. The listed false alarm metrics are:

1. PFA(MB) −− the probability that a "microburst" strength alarm from the WSP does not correlate with at least a "wind shear with loss";

18

2. PFA(LOSS) — — the corresponding probability for the combined categories of "wind shear with loss" and "microburst" alarms from the WSP;

3. P(OW) — — the probability that a "microburst" strength alarm from the WSP actually corresponds to a "wind shear with loss" and is therefore an "overwarning."

TABLE 2.
MICROBURST ALGORITHM PATH—ORIENTED SCORING STATISTICS

DETECTION PROBABILITY METRICS

P(LOSS | LOSS)	0.72
P(LOSS | MB)	0.97
P(MB | MB)	0.84

FALSE ALARM PROBABILITY METRICS

PFA (MB)	0.05
PFA (LOSS)	0.10
P(OW)	0.26

This analysis shows that while the probability for alarming a runway in the presence of microburst—strength shear (0.97) was consistent with the hit—miss analysis, the probability of correctly reporting the shear as a microburst—strength event was somewhat lower (0.84). Likewise, although the probability of generating a false microburst strength alarm in the absence of wind shear on a runway was low (0.05), a significant fraction (0.26) of these alarms corresponded to "wind shear with loss" and were therefore tabulated as "overwarning."

Appendix B contains a corresponding path—oriented scoring analysis that includes not only the actual runways at Orlando, but also a number of additional "imaginary" runways in order to extend the analysis to a larger geographic area and to different runway orientations with respect to the ASR—9 testbed. The appendix also gives corresponding performance metrics for the WSP when integrated with the enhanced LLWAS system at Orlando.

3.2 GUST FRONT DETECTION PERFORMANCE

Although operationally useful, the gust front algorithm implemented for the 1991 test failed to provide detection performance consistent with the quality of gust front signatures in the reflectivity and radial velocity "base" data from the WSP. As a result, a number of significant gust front events during the test period were missed, resulting in failure to provide advanced warning of a wind shift at the airport. Subsequent development of a more sophisticated "Machine Intelligent (MI)" [6] detection algorithm has confirmed that the WSP base data supports reliable automated gust front detection. This section includes performance measurements for the improved algorithm for comparison with that actually achieved during the operational demonstration.

19

The "Advanced Gust Front Algorithm (AGFA)" employed during the 1991 WSP test was initially developed for the TDWR and incorporates multiple "feature detectors" (i.e., convergent radial shear, reflectivity thin lines, convergent azimuthal shear) to improve detection relative to the baseline TDWR algorithm (which relies on radial shear detection alone). For TDWR−based gust front detection, however, the AGFA requires the presence of convergent radial shear along at least a part of the front in order to minimize false alarms from the additional feature detectors.

Reduced sensitivity associated with the elevation fan beam of the ASR−9 significantly reduces the WSP's capability to measure the convergent wind pattern associated with low reflectivity gust fronts. As a result, the WSP implementation of the AGFA relied solely on reflectivity thin line recognition and tracking. During shakedown prior to the operational demonstration, it was found that the thin line feature detector produced unacceptably high false−alarm rates (primarily associated with subtle reflectivity structures in stratiform precipitation); in the absence of a requirement that thin lines be associated with convergent velocity features, the end−to−end false alarm probability for the AGFA was likewise determined to be too high. Subsequent parameter adjustments to reduce the false−alarm probability resulted in a "detuning" of the algorithm and a significant reduction in its detection performance.

Table 3 tabulates the statistical performance of the AGFA for representative gust fronts during the operational test period. The analysis encompasses 15 hours of data and includes null cases to quantify false alarm probabilities. "Truth" was generated by a human interpreter examining the reflectivity and radial velocity images from the WSP: thus Table 3 excludes the effect of gust fronts whose signatures were simply not evident in WSP base data. The first two columns deal with simple recognition of the gust front signature; the second two tabulate the average fraction of the gust fronts' lengths that were identified by the algorithm. For comparison, performance of the "Machine Intelligent" (MI) gust front detection algorithm developed subsequent to the operational test is also shown.

TABLE 3.
GUST FRONT SIGNATURE DETECTION PERFORMANCE
(TRUTH BASED ON WSP DATA)

| | GUST FRONT SIGNATURES | | GUST FRONT LENGTH | |
	Prob. Detected	Prob. False	Frac. Detected	Frac. False
AGFA	0.56	0.05	0.38	0.15
MI	0.91	0.03	0.89	0.32

Table 4 repeats this analysis using "truth" derived from human examination of TDWR testbed base data. This tabulation assesses both the capability of the ASR−9 to measure a signature from the gust fronts, and the ability of the automated algorithm to recognize this signature. It is thus an end−to−end measure of the capability of the WSP to provide gust front detection and advanced warning.

20

TABLE 4.
WSP END-TO-END GUST FRONT DETECTION PERFORMANCE
(TRUTH BASED ON TDWR DATA)

	GUST FRONTS		GUST FRONT LENGTH	
	Prob. Detected	Prob. False	Frac. Detected	Frac. False
AGFA	0.40	0.07	0.18	0.07
MI	0.78	0.00	0.58	0.04

The tables emphasize that the gust front detection performance achieved during the operational test was suboptimal; the AGFA correctly identified the gust front on only 56% of the scans where a signature was in fact recognizable by a human analyst. This suboptimal detection performance, in combination with the approximately 15% of Orlando gust fronts that produced no visible thin line feature in the WSP base data, resulted in and end-to-end detection probability of only 0.4.

The machine-intelligent algorithm has produced markedly improved detection statistics in off-line testing. Over 90% of recognizable gust front signatures in the WSP data were automatically detected by the MI technique, and a corresponding fraction of their total length was identified. Comparison of Tables 3 and 4 shows that the MI algorithm's apparent high false-alarm probability with respect to fraction of length detected is, in fact, indicative of the algorithm's ability to detect segments of gust fronts not observed by the human truthers in the WSP data. (These segments are, however, tabulated in the TDWR "truth" set owing to the greater sensitivity of that radar.) The end-to-end gust front detection probability for the WSP using the MI approach was approximately 0.8; this is comparable to currently demonstrated TDWR performance.

3.3 SIX-LEVEL PRECIPITATION AND STORM MOTION ALGORITHM

These products were enthusiastically received by Orlando Air Traffic personnel. While no quantitative evaluations were performed, monitoring of these products during the operational test indicated that the information provided was accurate.

A significant change for the 1991 test was implementation of an anomalous propagation (AP) censoring function. False weather echoes resulting from ground clutter breakthrough associated with AP have been a significant operational problem in Air Traffic's utilization of the ASR-9's six-level weather reflectivity processor. When the WSP's censor function was activated (via a user controllable switch on the geographic situation display), the signal mean Doppler and spectrum width estimates for each radar resolution cell were tested in order to discriminate between true weather echoes and ground clutter breakthrough associated with AP.

Figure 6 illustrates the AP censoring function by means of GSD displays with the censor turned on and off. Cool, moist outflow air from a line of thunderstorms has resulted in ducting of radar energy to the surface and associated strong ground clutter to the west of Orlando's airport. With the mean Doppler/spectrum width test activated, most of the AP−induced ground clutter echoes are censored. Note that the display of true weather (in this example, the line of thunderstorms east of the airport) is not significantly altered by the censoring process.

Further work is underway to:

1. Implement spatial filtering to eliminate the speckled, AP breakthrough residue that remains after the censoring process;

2. Develop an interface to the ASR−9's Surveillance Communication Interface Processor (SCIP) that will allow the WSP to remove AP−induced false weather from the six−level ASR−9 weather display on controllers' DEDS.

3.4 FAA TECHNICAL CENTER AND AIR TRAFFIC CONTROLLER EVALUATIONS

A debrief meeting at the Orlando Air Traffic Control tower took place following completion of the operational test. Representatives from the FAA Technical Center (FAATC) and Orlando Air Traffic attended. Overall, the FAATC viewed the performance of the WSP as very good and stated that development and testing should continue. They noted that the gust front algorithm needed additional development since a number of clearly discernable gust front signatures were not detected by the algorithm used during the test period. A quick look report from FAATC [6] has been published for the 1991 operational test.

The Orlando Air Traffic (AT) personnel present confirmed statements made during the test period that, from AT's viewpoint, there were no significant differences between WSP performance and that observed during the preceding TDWR test. AT was enthusiastic about the performance of both systems over the summer and stated that algorithm refinements made as a result of the 1990 tests had largely eliminated their concerns about microburst "overwarning." At the close of the meeting, AT requested that either the WSP or TDWR (they didn't care which) continue to provide data to the tower when active weather affects the airport.

22
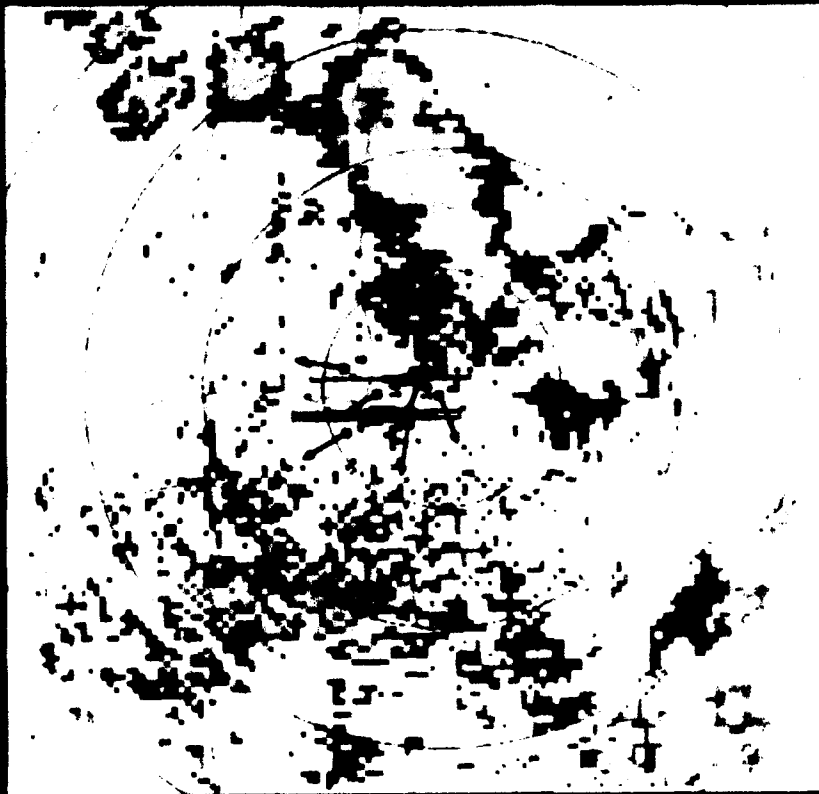
AP CENSOR ON

AP CENSOR OFF
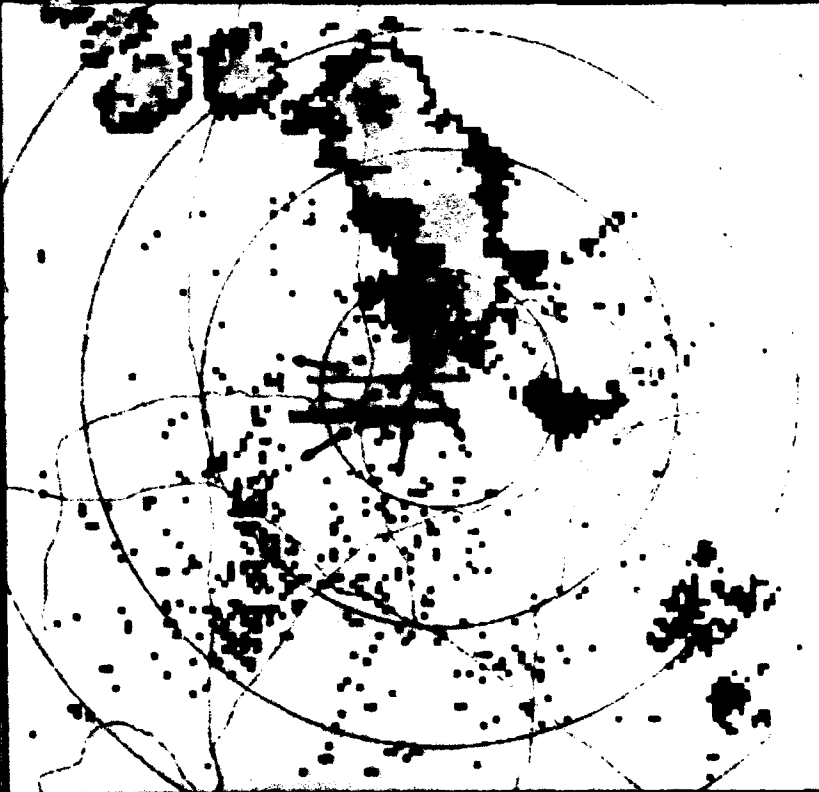
Figure 6. Example of WSP's anomalous propagation censoring function. Six-level precipitation reflectivity data are encoded as in Figure 4a.

23

4. SUMMARY AND FUTURE ACTIVITIES

The 1991 operational evaluation of the ASR–9 WSP provided a valuable opportunity to assess the system over an extended period of intense weather activity. System performance was consistent with previous evaluations of the WSP in the southeastern United States, confirming the capability for highly reliable detection of microbursts. Gust front detection during the test, while operationally useful, was not as reliable as it should have been, given the quality of gust front signatures in the base reflectivity and radial velocity data from the WSP. Subsequent development of a "Machine Intelligent" gust front algorithm has resulted in significantly improved detection capability.

A follow–on demonstration will take place during 1992 to complete validation of the WSP in the southeastern United States. Significant changes relative to the 1991 test will include:

1. Implementation of RF waveguide switches and couplers that allow the WSP to operate in parallel with the ASR–9's target and six–level weather processors. The 1992 test will therefore utilize a full–up emulation of production WSP radar interfaces;

2. Utilization of the Machine Intelligent gust front algorithm; and

3. On–line demonstration of the WSP operating in an integrated mode with Orlando's Enhanced LLWAS system. This demonstration is contingent on commissioning of the additional sensors required for the Enhanced LLWAS.

4. Utilization of refined algorithms for data quality editing (e.g., suppression of second–trip weather).

Following the 1992 demonstration, the WSP testbed will be moved to a midwest or High Plains airport for data collection and system evaluations in different environments. This activity will support national deployment of WSPs by providing the data base necessary to adjust processing algorithm parameters for differing storm structures encountered in the diverse meteorological regimes of the United States.

REFERENCES

1. Noyes, T., S. Troxel, M. Weber, O. Newell, J. Cullen, *The 1990 airport surveillance radar wind shear processor (ASR—WSP) operational test at Orlando International Airport*, Massachusetts Institute of Technology Lincoln Laboratory Project Report ATC—178, DOT—FAA—NR—91—1, 1991.

2. Weber, M., M. Stone, C. Primeggia, J. Anderson, Airport surveillance radar based wind shear detection, Preprint Volume: Fourth International Conference on Aviation Weather Systems, Paris, France, June 24—28, 1991, American Meteorological Society.

3. Evans, J. and D. Turnbull, *Development of an automated wind shear detection system using Doppler weather radar*, IEEE Proceedings, 77, 1661—1673, 1989.

4. Clark, M., Fisher, L. and J. Gibson, *Integrated windshear systems cost—benefit and deployment study*, Martin Marietta Report ATS—90—xxx, 1991.

5. Wilson, F.W, R. Gramzow, *The redesigned low level wind shear alert system*, Preprint Volume: Fourth International Conference on Aviation Weather Systems, Paris, France, June 24—28, 1991, American Meteorological Society.

6. Delanoy, R. and S. Troxel, *Machine intelligent gust front algorithm*, Massachusetts Institute of Technology Lincoln Laboratory Project Report, in preparation.

7. Martinez, R., *A quick—look report for the 1991 demonstration and operational test and evaluation of the airport surveillance radar wind shear processor (ASR—WSP) at Orlando International Airport in Orlando, Fla.*, FAA Technical Center Report CN—240—92—01, 1991.

8. Weber, M., *Dual—beam autocorrelation based wind estimates from airport surveillance radar signals*, Massachusetts Institute of Technology Lincoln Laboratory Project Report ATC—167, FAA—PS—89—5, 1989.

9. Chornoboy, E.S., *Doppler mean velocity estimation: small sample analysis and a new estimator*, Massachusetts Institute of Technology Lincoln Laboratory Technical Report TR—942, FAA—NR—92—5.

10. Cole, R., *Message Level TDWR/Enhanced LLWAS Integration Algorithm*, Massachusetts Institute of Technology Lincoln Laboratory Project Report, in preparation.

APPENDIX A
DATA PROCESSING ALGORITHMS

A.1 Signal Processing Algorithms

Figure A.1 diagrams the signal processing flow used during the 1991 test. Pulse samples from the high and low receiving beams were processed in parallel using 26-sample coherent processing intervals (CPIs): these consisted of two eight-pulse, low PRF blocks and one intervening 10-pulse, high PRF block from the ASR-9. Thus, the data processing intervals span 1.5 antenna beamwidths and successive azimuth samples overlap by 50%.
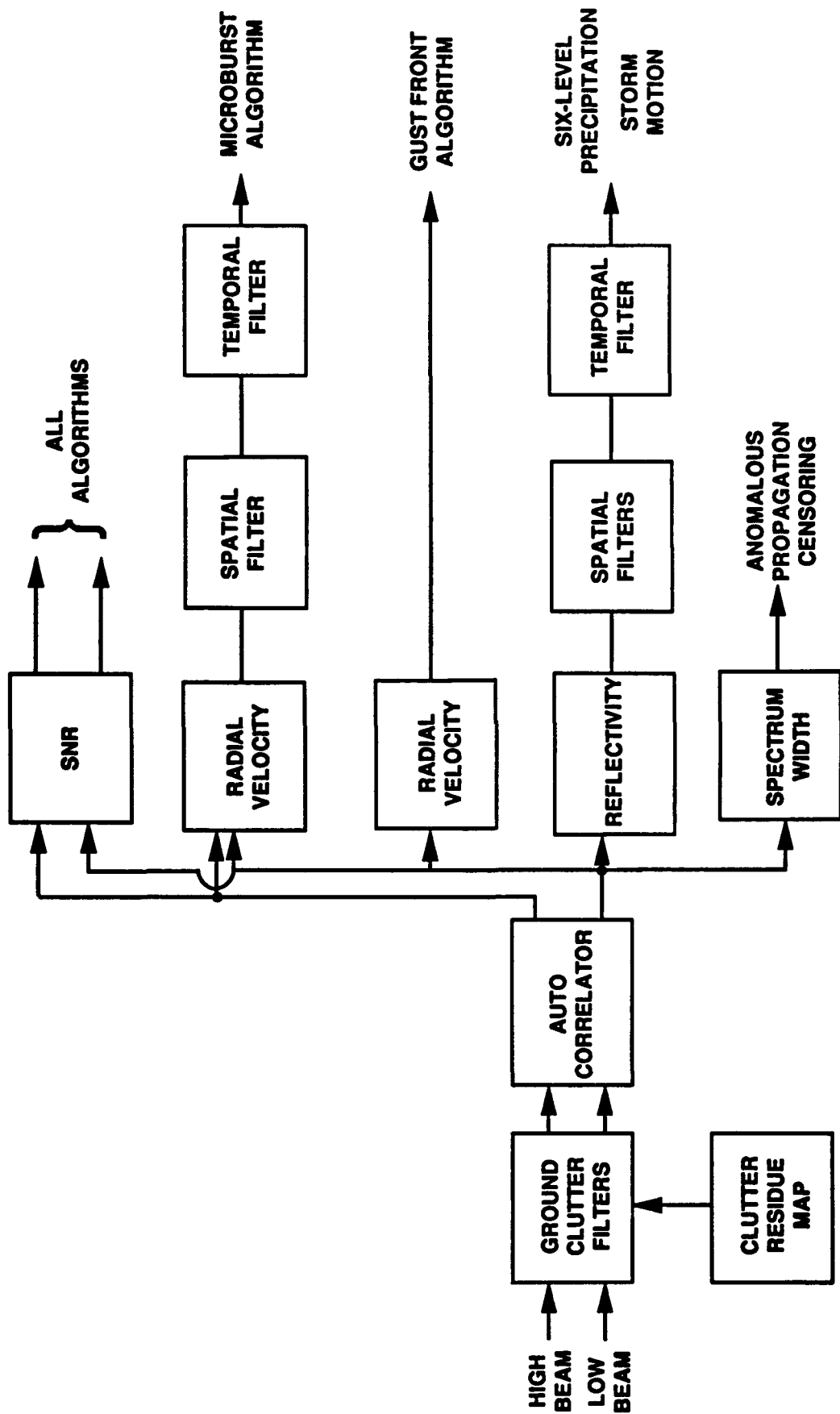
For each resolution cell, a map stores mean residual clutter power out of each of three 17-point finite impulse response (FIR) high-pass filters and an all-pass filter. The processor selects the least attenuating clutter filter that maintains signal-to-stored clutter residue power in excess of a 10 dB threshold. A "bad data" flag is set for resolution cells where the most attenuating filter output does not exceed this threshold. Clutter suppression for the three FIR filters varied from 12 to 50 dB.

Autocorrelation function estimates for lags varying from zero to four times the average pulse repetition interval ($R(0)$ through $R(4)$) were computed for both beams and used to compute the weather echo spectrum moments estimates used by the meteorological detection algorithms. Signal-to-noise power ratio (SNR) and the precipitation reflectivity factor were computed using $R(0)$ and a stored estimate for the system noise level in each beam receiving channel. The Doppler velocity estimate supplied to the gust front algorithm was computed using the phase angle of the low-beam $R(1)$ estimate. The microburst algorithm employed a Doppler velocity field derived through combination of low- and high-beam $R(0)$ and $R(1)$ estimates in order to cancel signal contributions not associated with winds near the surface [8]. Spectrum width was calculated for the low beam using a weighted, quadratic regression to the logarithms of the magnitudes of $R(0)$ through $R(4)$. [9]
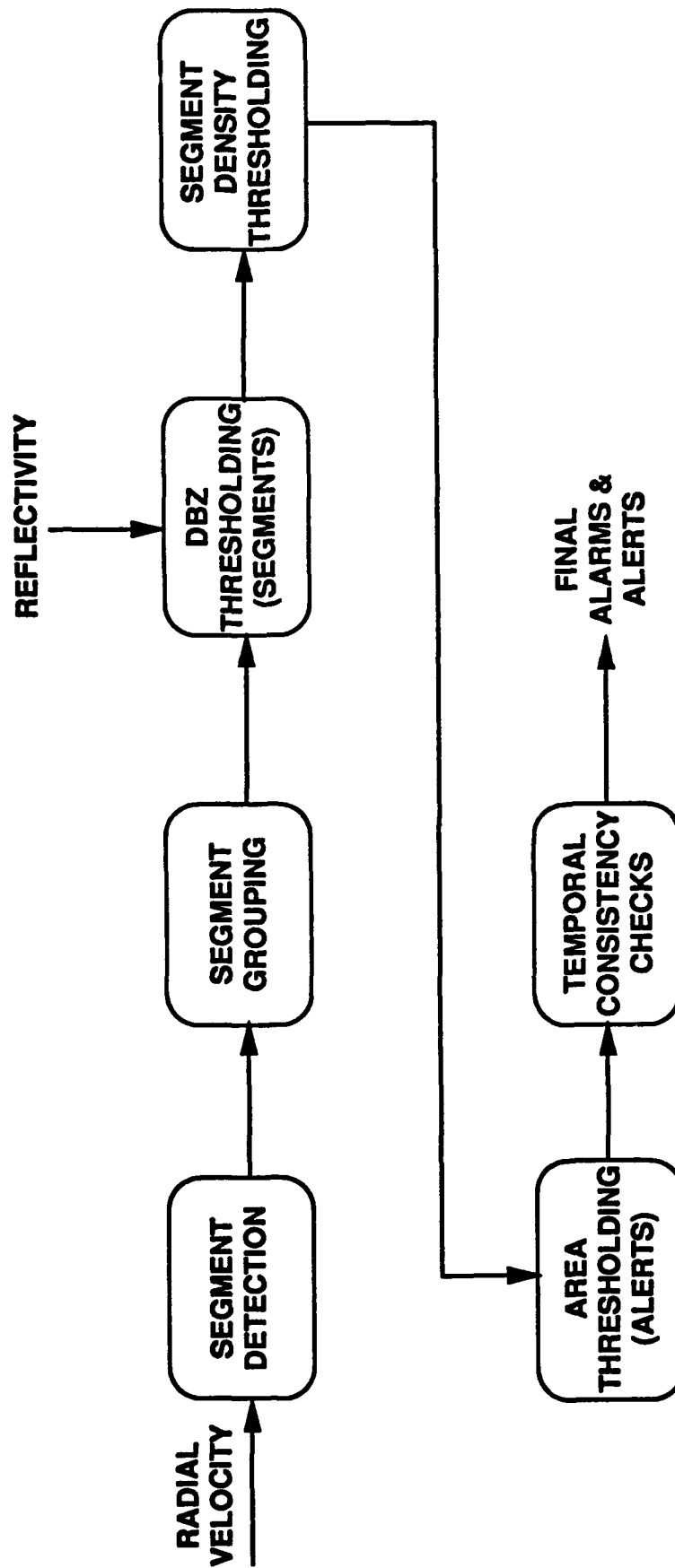
A.2 Microburst Detection Algorithm

Figure A.2 is a block diagram of the microburst detection algorithm. The Doppler velocity field is searched radial by radial for the characteristic increasing velocity signature associated with divergent outflows. The endpoints of these "shear segments" are recursively averaged from scan to scan. The segments are then grouped azimuthally into "clusters." Since Orlando microbursts are essentially always associated with heavy precipitation, the likelihood of false alarms was reduced by discarding segments that are too far from regions of significant reflectivity (30 dBz).

The initial segment grouping operation skips over missing segments (up to a maximum number set by algorithm parameters). The segment density threshold prevents this process from generating large regions of low segment density, for example, in noisy or weak shear portions of the velocity field. A filter passed over the segments azimuthally is used to calculate segment density for this thresholding process.

29

A.1. Signal processing block diagram.

RADIAL
VELOCITY → SEGMENT DETECTION → SEGMENT GROUPING → DBZ THRESHOLDING (SEGMENTS) → SEGMENT DENSITY THRESHOLDING

REFLECTIVITY → DBZ THRESHOLDING (SEGMENTS)

SEGMENT DENSITY THRESHOLDING → AREA THRESHOLDING (ALERTS) → TEMPORAL CONSISTENCY CHECKS → FINAL ALARMS & ALERTS

A.2.   Microburst detection algorithm block diagram.

Minimum area thresholds (functions of range and alarm strength) are then applied, followed by scan-to-scan consistency checks. Before being output to user displays, a microburst is required to have been detected on at least three scans (15 seconds). Once established, an alarm will not be cancelled until detection has ceased for 12 successive scans (1 minute).

A.3 Gust Front Detection Algorithm

The "Advanced Gust Front Algorithm" used for the 1991 WSP test consists of three stages:

1. Reflectivity thin line feature extraction;
2. Feature association and discrimination; and
3. Wind shift and wind shear estimation.

The feature extractor utilizes a successive thresholding scheme to extract segments associated with localized "ridges" in the reflectivity field. Segments are generated in two passes through the reflectivity field. The first pass constructs segments along radials (constant azimuth) and the second along arcs of constant range. Up to 10 fixed threshold levels are used to extract the segments. Once generated, the segments are associated by means of spatial proximity tests to generate thin line features. The final features passed to the association and discrimination module consist of lists of points connecting the midpoints of detected reflectivity ridges.

The association and discrimination stage uses a rule base, coupled with spatial and temporal association tests, to combine potentially fragmented thin line features into gust front detections, and to reject features not associated with actual fronts. A track history is formed for detected gust fronts and used to generate forecasts of future gust front positions.

The wind shift/shear estimation module generates an estimate of the wind speed and direction behind the gust front and the change in wind speed across the front. The estimate of wind speed behind the front is derived using the WSP's Doppler velocity measurements in the reflectivity thin line region; post-frontal wind direction is set equal to the propagation direction of the thin line. Prefrontal wind speed and direction (necessary in generating wind shear estimates) is taken as the LLWAS network mean wind velocity prior to the front's arrival at the airport.

A.4 Storm Tracking Algorithm

The storm motion algorithm uses scan-to-scan correlation of the WSP's reflectivity measurements to estimate the speed and direction of storm movement. The reflectivity images are thresholded to produce binary representations of storm cells. These are partitioned into "correlation boxes" (typically 10 km x 10 km). For each box, a scan-to-scan displacement vector is computed by finding that displacement which maximizes the cross correlation between scans N and N-1. The uniform grid of displacement vectors so derived is smoothed spatially (nine-point median filter) and temporally (single-pole recursive filter).

The final stage of processing is an analysis of the original reflectivity image to identify local maxima corresponding to distinct storm cells. The closest gridded displacement vector is used to generate the speed and direction estimate for each identified cell.

A.5 Anomalous Propagation Censoring

Anomalous propagation conditions result in ground clutter more intense than the values stored in the signal processor's clutter residue map. When this occurs, inadequate clutter suppression is invoked and the reflectivity and Doppler estimates are contaminated by clutter breakthrough. This condition is flagged by testing the mean Doppler and spectrum width of the (post clutter filtered) signal to discriminate between true weather echoes and AP−induced ground clutter breakthrough. While precipitation echoes may have a low mean Doppler velocity (for example, when moving tangential to the radar's beam) their spectrum width is almost always significantly broader than that of antenna scan modulated ground clutter owing to turbulence and vertical shear within the ASR−9's fan elevation beam. The AP censor flag was set "true" in resolution cells where signal spectrum width was less than 2 m/s and the mean Doppler velocity was less than 1 m/s. This binary field of censor flags was then smoothed along the range axis using an M−of−N filter.

APPENDIX B
## OFF-LINE EVALUATION OF ASR-9 WSP/ENHANCED LLWAS INTEGRATION

The path-oriented scoring methodology described in Section 3.1 was used to perform an off-line evaluation of the microburst detection performance of the ASR-9 WSP operating in an integrated mode with an Enhanced LLWAS system. The extended anemometer network consisting of the Lincoln Laboratory MESONET and Orlando's 15-station enhanced LLWAS was used to measure the detection performance of an integrated system on both the actual runways at MCO and a large set of imaginary runways. Use of the imaginary runways significantly increased the number of wind shear events included in the analysis and allowed for scoring of microburst events at ranges up to 16 km from the ASR-9 and for runways at a variety of orientation angles with respect to the radar. Figure B.1 plots the locations of the anemometers and the real and imaginary runways used for the analysis.

The integration algorithm evaluated was the "message level" [10] algorithm developed at Lincoln Laboratory to accomplish TDWR/Enhanced LLWAS integration. Briefly, the algorithm compares the runway-specific alphanumeric alarms generated by both systems to derive the integrated product. Strong microburst detections (loss > 30 kts) from either system are passed through by the integration algorithm whereas weaker events are required to satisfy various consistency checks. The wind speed loss estimate is taken as the average of the two input loss estimates unless that average is less than 80% of the stronger input; in this latter case, the reported loss is 80% of the stronger input.

Table B.1 lists path-oriented microburst detection and false-alarm statistics for the stand-alone ASR-9 WSP, stand-alone enhanced LLWAS, and integrated system. The performance metrics were defined in Section 3.1. Scoring for the imaginary runway corridors accounts for the slight discrepancies in ASR-9 WSP stand-alone performance relative to Table 2.

TABLE B.1
WSP/LLWAS MICROBURST DETECTION PERFORMANCE

	ASR-9	ENHANCED LLWAS	INTEGRATED
DETECTION PROBABILITY METRICS			
P(LOSS | LOSS)	0.65	0.73	0.82
P(LOSS | MB)	0.97	0.99	0.99
P(MB | MB)	0.86	0.90	0.94
FALSE ALARM PROBABILITY METRICS			
PFA (MB)	0.03	0.0	0.02
PFA (LOSS)	0.09	0.01	0.07
P(OW)	0.22	0.23	0.22

35
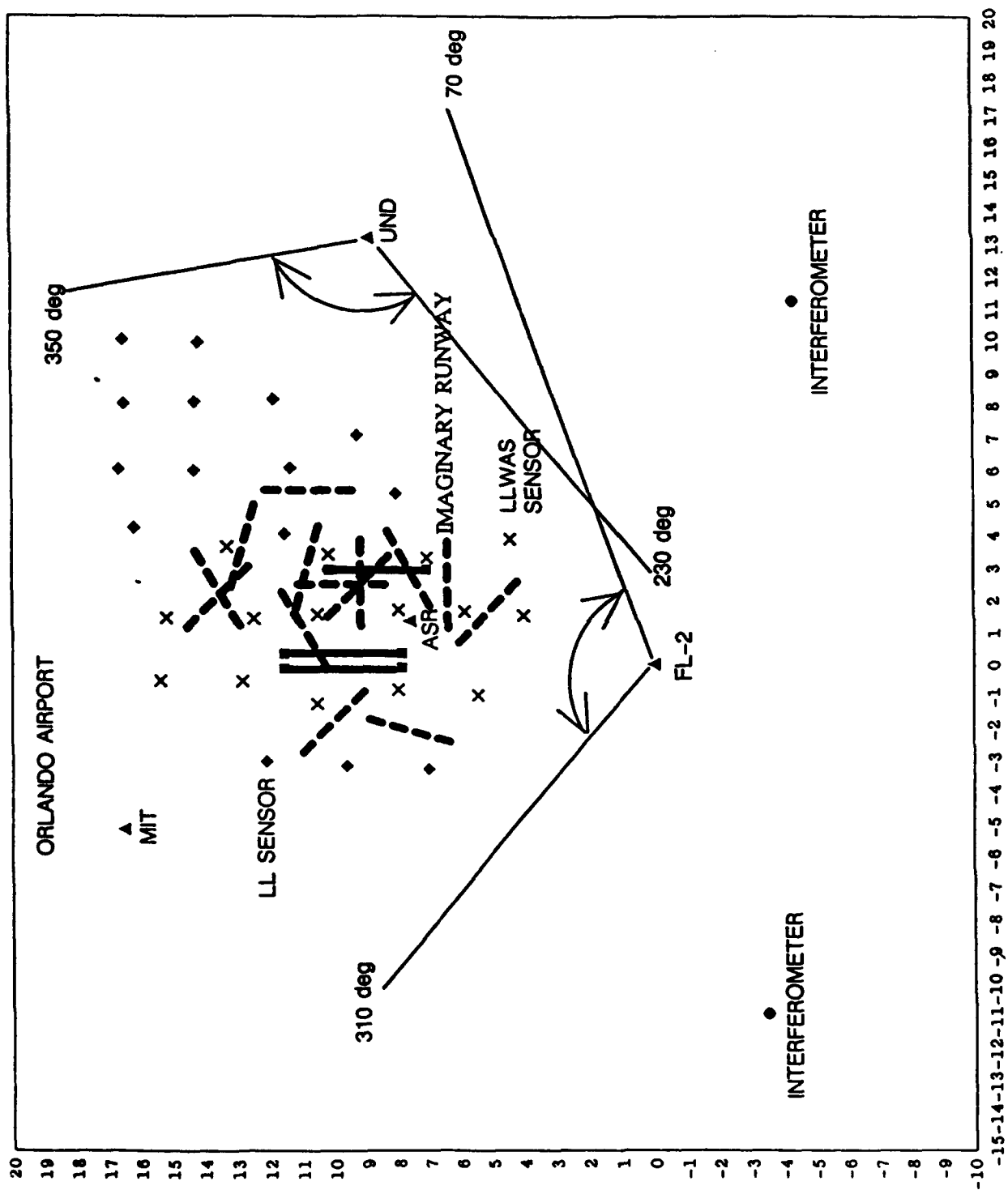
B.1. Locations of anemometers and runways (real and imaginary) used for analysis of ASR-9 WSP/Enhanced LLWAS integration algorithm.

This scoring indicates two benefits for the integrated system. The probability of detecting a weak microburst ("wind shear with loss") was increased significantly relative to either system stand–alone, as was the probability of correctly reporting a "microburst strength loss" (> 30 kts) as a microburst.